Chemistry of *C*-Trimethylsilyl-Substituted Main-Group Heterocarboranes. 4. Reactivity of Stannacarboranes toward Monodentate and Bis(bidentate) Lewis Bases. Syntheses and Structures of 1- or 1,1′-(L)-[*closo*-1-Sn-2-($SiMe_3$)-3-(R)-2,3-$C_2B_4H_4$]$_n$ {*n* = 1, L = [(η^5-C_5H_5)Fe(η^5-$C_5H_4CH_2(CH_3)_2N$)]; *n* = 2, L = 2,2′-$C_8H_6N_4$; R = $SiMe_3$, Me, or H}

Narayan S. Hosmane,* Joseph S. Fagner, Hong Zhu, Upali Siriwardane, John A. Maguire, Guomin Zhang, and Brian S. Pinkston

Department of Chemistry, Southern Methodist University, Dallas, Texas 75275

Received December 23, 1988

The *closo*-stannacarboranes 1-Sn-2,3-($SiMe_3$)$_2$-2,3-$C_2B_4H_4$ (I), 1-Sn-2-($SiMe_3$)-3-(Me)-2,3-$C_2B_4H_4$ (II), and 1-Sn-2-($SiMe_3$)-2,3-$C_2B_4H_5$ (III) react somewhat slowly with (ferrocenylmethyl)-*N*,*N*-dimethylamine and almost instantaneously with 2,2′-bipyrimidine in dry benzene to form donor–acceptor complexes 1-Sn[(η^5-C_5H_5)Fe(η^5-$C_5H_4CH_2(Me)_2N$)]-2,3-($SiMe_3$)$_2$-2,3-$C_2B_4H_4$ (IV), 1-Sn[(η^5-C_5H_5)Fe(η^5-$C_5H_4CH_2$-$(Me)_2N$)]-2-($SiMe_3$)-3-(Me)-2,3-$C_2B_4H_4$ (V), and 1-Sn[(η^5-C_5H_5)Fe(η^5-$C_5H_4CH_2(Me)_2N$)]-2-($SiMe_3$)-2,3-$C_2B_4H_5$ (VI) and 1,1′-(2,2′-$C_8H_6N_4$)-[*closo*-1-Sn-2,3-($SiMe_3$)$_2$-2,3-$C_2B_4H_4$]$_2$ (VII), 1,1′-(2,2′-$C_8H_6N_4$)-[*closo*-1-Sn-2-($SiMe_3$)-3-(Me)-2,3-$C_2B_4H_4$]$_2$ (VIII), and 1,1′-(2,2′-$C_8H_6N_4$)-[*closo*-1-Sn-2-($SiMe_3$)-2,3-$C_2B_4H_5$]$_2$ (IX) in yields ranging from 61 to 81%. These complexes IV–IX were characterized on the basis of ^1H, ^{11}B, ^{13}C, and ^{119}Sn NMR spectra and IR spectra and where possible by mass spectroscopy and elemental analyses. Complexes IV and VII were also characterized by single-crystal X-ray diffraction. The structure of IV shows two crystallographically independent molecules in the unit cell. Both show the apical tin atoms are slightly slipped toward the boron side of the carborane C_2B_3 face with the Sn–N bond being directly over the unique boron in one molecule, while in the other molecule it is slightly rotated away from this boron. In both molecules, the ferrocenyl group of the Lewis base is not in a position of minimum steric interactions with the stannacarborane but is oriented in such a way that the lower half of the cyclopentadienyl ring is within the van der Waals distances to the cage. The coordination geometry of each tin in VII is quite similar to that found in other donor–acceptor complexes of the stannacarboranes. MNDO–SCF calculations on the model compound 1,1′-(2,2′-$C_8H_6N_4$)-[*closo*-1-Sn-2,3-$C_2B_4H_6$]$_2$ indicated that the trans configuration in VII is due to steric interactions. Compound IV crystallizes in the triclinic space group $P\bar{1}$ with a = 12.710 (3) Å, b = 14.329 (5) Å, c = 17.443 (6) Å, α = 102.59 (3)°, β = 97.48 (3)°, γ = 110.00 (3)°, U = 2839.9 (15) Å^3, and Z = 4. Full-matrix least-squares refinement converged at R = 0.060 and R_w = 0.068. Compound VII crystallizes in the monoclinic space group $P2_1/c$ with a = 15.884 (4) Å, b = 9.841 (3) Å, c = 13.550 (4) Å, β = 104.71 (2)°, U = 2048.4 (9) Å^3, and Z = 2. The structure was refined to R = 0.059 and R_w = 0.076.

Introduction

Several reviews that summarize the preparative chemistry and structural investigations of the main group heterocarboranes have recently appeared.[1,2] It has been established that the capping group 14 heteroatoms in the closo complexes all have a lone pair of electrons exo to the cage, but there is very little evidence that these lone pairs are chemically active. With the exception of [$GeCB_{10}H_{11}$]$^-$, an anionic germanium compound reported by Todd et al.,[3] the group 14 heterocarboranes show no tendency to react with Lewis acids.[4-6] On the contrary, the heterocarboranes form donor–acceptor complexes with Lewis bases with group 14 atoms acting as acid sites. The most studied are the stannacarboranes (see Scheme I). Structures have been determined for the 2,2′-bipyridine complexes ($C_{10}H_8N_2$)Sn($SiMe_3$)(R)$C_2B_4H_4$[7,8] (R = $SiMe_3$ or Me) and ($C_{10}H_8N_2$)Sn$(Me)_2C_2B_9H_9$[9,10] and a tetrahydrofuran complex, (C_4H_8O)Sn$(Me)_2C_2B_9H_9$.[10] The structure of the complex of 1-Sn-2-($SiMe_3$)-3-(Me)-2,3-$C_2B_4H_4$ with the tridentate Lewis base 2,2′:6′,2″-terpyridine has also been reported.[11] All show an extreme slippage of the tin toward the boron side of the C_2B_3 face in such a way that the tin could be considered to be η^3 bonded to the carborane. The slippage of the apical tin in the THF complex is significantly less than that observed for the corresponding 2,2′-bipyridine analogue. In our recent preliminary communication,[12] it has been shown that the stannacarboranes form exclusively bridged donor–acceptor complexes with 2,2′-bipyrimidine. However, the factors that dictate the

(1) Hosmane, N. S.; Maguire, J. A. *Molecular Structure and Energetics*; Greenberg, A., Liebman, J. F., Williams, R. E., Eds.; VCH: New York, 1988; Vol. 5, Chapter 14, pp 297–328.
(2) Hosmane, N. S.; Maguire, J. A. *Adv. Organomet. Chem.* **1989**, *30*, 0000.
(3) (a) Wikholm, G. S.; Todd, L. J. *J. Organomet. Chem.* **1974**, *71*, 219. (b) Todd, L. J.; Burke, A. R.; Silverstein, H. T.; Little, J. L.; Wikholm, G. S. *J. Am. Chem. Soc.* **1969**, *91*, 3376.
(4) (a) Voorhees, R. L.; Rudolph, R. W. *J. Am. Chem. Soc.* **1969**, *91*, 2173. (b) Rudolph, R. W.; Voorhees, R. L.; Cochoy, R. E. *J. Am. Chem. Soc.* **1970**, *92*, 3351. (c) Chowdhry, V.; Pretzer, W. R.; Rai, D. N.; Rudolph, R. W. *J. Am. Chem. Soc.* **1973**, *95*, 4560.
(5) Wong, K.-S.; Grimes, R. N. *Inorg. Chem.* **1977**, *16*, 2053.
(6) Hosmane, N. S.; Sirmokadam, N. N.; Herber, R. H. *Organometallics* **1984**, *3*, 1665.
(7) Hosmane, N. S.; de Meester, P.; Maldar, N. N.; Potts, S. B.; Chu, S. S. C.; Herber, R. H. *Organometallics* **1986**, *5*, 772.
(8) Siriwardane, U.; Hosmane, N. S.; Chu, S. S. C. *Acta Crystallogr., Sect. C: Cryst. Struct. Commun.* **1987**, *C43*, 1067.
(9) Cowley, A. H.; Galow, P.; Hosmane, N. S.; Jutzi, P.; Norman, N. C. *J. Chem. Soc., Chem. Commun.* **1984**, 1564.
(10) Jutzi, P.; Galow, P.; Abu-Orabi, S.; Arif, A. M.; Cowley, A. H.; Norman, N. C. *Organometallics* **1987**, *6*, 1024.
(11) Siriwardane, U.; Hosmane, N. S. *Acta Crystallogr., Sect. C: Cryst. Struct. Commun.* **1988**, *C44*, 1572.
(12) Hosmane, N. S.; Islam, M. S.; Siriwardane, U.; Maguire, J. A.; Campana, C. F. *Organometallics* **1987**, *6*, 2447.

0276-7333/89/2308-1769$01.50/0

Scheme I

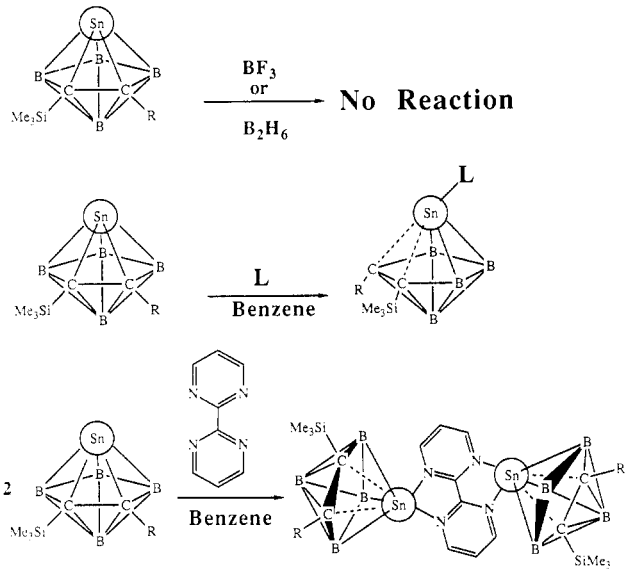

R = Me_3Si , Me , H
B = BH
L = Mono-, Bi-, or Tri-dentate Lewis Base

trans configuration of the two stannacarboranes in the bridged complex were not addressed. To date, it is not known whether stannacarboranes would form stable donor–acceptor complexes with monodentate Lewis bases other than THF and whether this complexation would result in any drastic changes in the bonding of the metal to the C_2B_3 face of the carborane fragment. Here we describe, in detail, the syntheses and characterizations of (ferrocenylmethyl)-*N*,*N*-dimethylamine and 2,2′-bipyrimidine complexes of *C*-trimethylsilyl-substituted η^5-*closo*-stannacarboranes. In addition to MNDO–SCF calculations on the bridged complexes, the single-crystal X-ray analyses of 1-((ferrocenylmethyl)-*N*,*N*-dimethylamine)-2,3-bis(trimethylsilyl)-2,3-dicarba-1-stanna-*closo*-heptaborane(6) and 1,1′-(2,2′-bipyrimidine)-2,2′,3,3′-tetrakis(trimethylsilyl)-[bis(2,3-dicarba-1-stanna-*closo*-heptaborane)](12) will be presented in detail.

Experimental Section

Materials. 2,3-Bis(trimethylsilyl)-2,3-dicarba-1-stanna-*closo*-heptaborane(6), 2-(trimethylsilyl)-3-methyl-2,3-dicarba-1-stanna-*closo*-heptaborane(6), and 2-(trimethylsilyl)-2,3-dicarba-1-stanna-*closo*-heptaborane(6) were prepared by the methods of Hosmane et al.[6,13] Prior to use, 2,2′-bipyrimidine (Aldrich Chemical Co., Milwaukee, WI) was sublimed in vacuo, and (ferrocenylmethyl)-*N*,*N*-dimethylamine (Strem Chemicals, Inc., Newburyport, MA) was distilled in vacuo. Purity was checked by IR, NMR, and mp/bp measurements. Benzene and *n*-hexane were dried over $LiAlH_4$ and double distilled before use. All other solvents were dried over 4–8 mesh molecular sieves (Davidson) and either saturated with dry argon or degassed before use.

Spectroscopic Procedures. Proton, boron-11, carbon-13, silicon-29, and tin-119 pulse Fourier transform NMR spectra, at 200, 64.2, 50.3, 39.76, and 74.63 MHz, respectively, were recorded on an IBM-200 SY multinuclear NMR spectrometer. Mass spectral data were obtained on a Hewlett Packard GC/MS system 5988A. Infrared spectra were recorded on a Perkin-Elmer Model 283 infrared spectrometer and a Perkin-Elmer Model 1600 FT-IR spectrophotometer. Elemental analyses were obtained from Galbraith Laboratories, Knoxville, TN.

Synthetic Procedures. All experiments were carried out in Pyrex glass round-bottom flasks of 250-mL capacity, containing magnetic stirring bars and fitted with high vacuum Teflon valves. Nonvolatile substances were manipulated in either drybox or evacuable glovebags under an atmosphere of dry nitrogen. All known compounds among the products were identified by comparing their infrared and ^1H NMR spectra with those of authentic samples.

Synthesis of 1-Sn[(η^5-C_5H_5)Fe(η^5-$C_5H_4CH_2(Me)_2N$)]-2-($SiMe_3$)-3-(R)-2,3-$C_2B_4H_4$ (R = $SiMe_3$, Me, and H). 1-Sn-2,3-$(SiMe_3)_2$-2,3-$C_2B_4H_4$ (I) (0.84 g, 2.50 mmol), 1-Sn-2-($SiMe_3$)-3-(Me)-2,3-$C_2B_4H_4$ (II) (0.15 g, 0.54 mmol), or 1-Sn-2-($SiMe_3$)-2,3-$C_2B_4H_5$ (III) (0.25 g, 0.95 mmol) was dissolved in freshly distilled dry benzene (15 mL) in vacuo. This solution was then filtered through a frit under high vacuum onto freshly distilled (anhydrous) (ferrocenylmethyl)-*N*,*N*-dimethylamine, (η^5-C_5H_5)Fe(η^5-$C_5H_4CH_2(Me)_2N$) (0.16 g, 2.50 mmol; 0.13 g, 0.54 mmol; or 0.24 g, 0.95 mmol; when I, II, or III was used), contained in a 250-mL round-bottom flask maintained at −78 °C. When the reaction flask was warmed to 0 °C, the bright orange color of the mixture turned to deep red and the solution became turbid slowly. This mixture was constantly stirred for 4 h at 0 °C during which time, no gas evolution was detected. The solvent, benzene, and a trace quantity of unreacted (ferrocenylmethyl)-*N*,*N*-dimethylamine were then removed by pumping the reaction mixture over a period of 18 h in vacuo at room temperature to collect a bright orange gummy solid in the flask. This gummy solid was then washed in vacuo repeatedly with dry *n*-hexane (~20 mL) and then vacuum dried and recrystallized in dry benzene to isolate yellow-orange plates of 1-Sn[(η^5-C_5H_5)Fe(η^5-$C_5H_4CH_2(Me)_2N$)]-2,3-$(SiMe_3)_2$-2,3-$C_2B_4H_4$ (IV) (1.17 g, 2.02 mmol; 81% yield based on I consumed), orange needles of 1-Sn[(η^5-C_5H_5)Fe(η^5-$C_5H_4CH_2(Me)_2N$)]-2-($SiMe_3$)-3-(Me)-2,3-$C_2B_4H_4$ (V) (0.17 g, 0.33 mmol; 61% yield based on II consumed), or yellow plates of 1-Sn[(η^5-C_5H_5)Fe(η^5-$C_5H_4CH_2(Me)_2N$)]-2-($SiMe_3$)-2,3-$C_2B_4H_5$ (VI) (0.37 g, 0.72 mmol; 76% yield based on III consumed).

The physical properties and characterization of IV are as follows: mp 91–92.5 °C; air and moisture sensitive; at 25 °C, highly soluble in benzene, THF, and $CHCl_3$ and sparingly soluble in dry *n*-pentane and *n*-hexane; ^1H NMR (C_6D_6, relative to external Me_4Si) δ 5.35 [q(br), 1 H, basal H_t, $^1J(^1H-^{11}B)$ = 130 Hz], 4.45 [q(br), 2 H, basal H_t, $^1J(^1H-^{11}B)$ = 121 Hz], 4.06 [s, 4 H, C_5H_4], 3.97 [s, 5 H, C_5H_5], 3.28 [s, 2 H, CH_2], 2.60 [q(br), 1 H, apical H_t, $^1J(^1H-^{11}B)$ = 152 Hz], 1.91 [s, 6 H, $N(Me)_2$], 0.51 [s, 18 H, $SiMe_3$]; ^{11}B NMR (C_6D_6, relative to external BF_3·OEt_2) δ 26.81 [d, 1 B, basal BH, $^1J(^{11}B-^1H)$ = 131.9 Hz], 21.18 [d, 2 B, basal BH, $^1J(^{11}B-^1H)$ = 120.6 Hz)], −11.14 [d, 1 B, apical BH, $^1J(^{11}B-^1H)$ = 154.2 Hz]; ^{13}C NMR (C_6D_6, relative to external Me_4Si) δ 136.38 [s(br), cage carbons (SiCB)], 80.09 [s, ferrocenyl carbon], 70.92 [d, 4 CH, C_5H_4, $^1J(^{13}C-^1H)$ = 175.71 Hz], 68.91 [d, 5 CH, C_5H_5, $^1J(^{13}C-^1H)$ = 177.55 Hz], 50.70 [t, CH_2, $^1J(^{13}C-^1H)$ = 136.62 Hz], 44.27 [q, $N(Me)_2$, $^1J(^{13}C-^1H)$ = 135.22 Hz], 2.57 [q, $SiMe_3$, $^1J(^{13}C-^1H)$ = 119.44 Hz]; ^{119}Sn NMR (C_6D_6, relative to external TMT) δ −79.18 [s(br), cage–Sn–L]. Anal. Calcd for $C_{21}H_{39}B_4NSi_2FeSn$: C, 43.55; H, 6.79; N, 2.42; B, 7.46; Si, 9.70; Fe, 9.64; Sn, 20.49. Found: C, 42.97; H, 6.75; N, 2.44; B, 6.32; Si, 6.94; Fe, 9.55; Sn, 20.98.

The physical properties and characterization of V are as follows: mp 147 °C dec; sensitive to air and moisture; at 25 °C, highly soluble in benzene, THF, and $CHCl_3$ and sparingly soluble in dry *n*-pentane and *n*-hexane; ^1H NMR (C_6D_6, relative to external Me_4Si) δ 4.57 [q(br), 1 H, basal H_t, $^1J(^1H-^{11}B)$ = 132 Hz], 4.04 [s, 4 H, C_5H_4], 3.93 [s, 5 H, C_5H_5], 3.66 [q(br), 2 H, basal H_t, $^1J(^1H-^{11}B)$ = 129 Hz], 3.17 [s, 2 H, CH_2], 2.62 [s, 3 H, C(cage)–Me], 2.46 [q(br), 1 H, apical H_t, $^1J(^1H-^{11}B)$ = 146 Hz], 2.03 [s, 6 H, $N(Me)_2$], 0.19 [s, 9 H, $SiMe_3$]; ^{11}B NMR (C_6D_6, relative to external BF_3·OEt_2) δ 25.64 [d, 1 B, basal BH, $^1J(^{11}B-^1H)$ = 132.78 Hz], 16.30 [d, 2 B, basal BH, $^1J(^{11}B-^1H)$ = 128.49 Hz], −10.48 [d, 1 B, apical BH, $^1J(^{11}B-^1H)$ = 145.63 Hz]; ^{13}C NMR (relative to external Me_4Si) δ 135.35 [s(br), cage carbon (SiCB)], 133.88 [s(br), cage carbon (CCB)], 83.12 [s, ferrocenyl carbon], 69.95 [d, 4 CH, C_5H_4, $^1J(^{13}C-^1H)$ = 166.46 Hz], 68.28 [d, 5 CH, C_5H_5, $^1J(^{13}C-^1H)$ = 177.56 Hz], 59.28 [t, CH_2, $^1J(^{13}C-^1H)$ = 135.02 Hz], 44.82 [q, $N(Me)_2$, $^1J(^{13}C-^1H)$ = 135.0 Hz], 23.08 [q, C(cage)–Me, $^1J(^{13}C-^1H)$ = 127 Hz], 0.78 [q(br), $SiMe_3$, $^1J(^{13}C-^1H)$ = 119.5 Hz]; ^{119}Sn NMR (C_6D_6, relative to external TMT) δ −25.01 [s(br), cage–Sn–L].

The physical properties and characterization of VI are as follows: mp 142 °C dec; sensitive to air and moisture; at 25 °C,

(13) Islam, M. S.; Siriwardane, U.; Hosmane, N. S.; Maguire, J. A.; de Meester, P.; Chu, S. S. C. *Organometallics* **1987**, *6*, 1936.

highly soluble in benzene, THF, and $CHCl_3$ and sparingly soluble in dry *n*-pentane and *n*-hexane; ^1H NMR ($CDCl_3$, relative to external Me_4Si) δ 6.89 [s(br), 1 H, cage CH], 4.23 [q(br), 1 H, basal H_t, $^1J(^1H-^{11}B)$ = 134 Hz], 4.11 [s, 4 H, C_5H_4], 4.05 [s, 5 H, C_5H_5], 3.43 [q(br), 2 H, basal H_t, $^1J(^1H-^{11}B)$ = 119 Hz], 3.31 [s, 2 H, CH_2], 2.57 [q(br), 1 H, apical H_t, $^1J(^1H-^{11}B)$ = 146.0 Hz], 2.12 [s, 6 H, $N(Me)_2$], 0.19 [s, 9 H, $SiMe_3$]; ^{11}B NMR ($CDCl_3$, relative to external $BF_3{\cdot}OEt_2$] δ 25.51 [d, 1 B, basal BH, $^1J(^{11}B-^1H)$ = 133.76 Hz], 16.22 [d, 2 B, basal BH, $^1J(^{11}B-^1H)$ = 119.37 Hz], −7.53 [d, 1 B, apical BH, $^1J(^{11}B-^1H)$ = 145.62 Hz]; ^{13}C NMR ($CDCl_3$ relative to external Me_4Si) δ 129.83 [s(br), cage carbon (SiCB)], 119.47 [d, cage CH, $^1J(^{13}C-^1H)$ = 170.84 Hz], 81.63 [s, ferrocenyl carbon], 70.32 [d, 4 CH, C_5H_4, $^1J(^{13}C-^1H)$ = 173.77 Hz], 68.47 [d, 5 CH, C_5H_5, $^1J(^{13}C-^1H)$ = 175.44 Hz], 58.95 [t, CH_2, $^1J(^{13}C-^1H)$ = 134.88 Hz], 44.61 [q, $N(Me)_2$, $^1J(^{13}C-^1H)$ = 134.24 Hz], 0.93 [q(br), $SiMe_3$, $^1J(^{13}C-^1H)$ = 117.85 Hz]; ^{119}Sn NMR ($CDCl_3$, relative to TMT) δ −28.39 [s(br), cage–Sn–L].

Synthesis of 1,1′-(2,2′-$C_8H_6N_4$)-[*closo*-1-Sn-2-($SiMe_3$)-3-(R)-2,3-$C_2B_4H_4$]$_2$ (R = $SiMe_3$, Me, and H). In a procedure identical with that employed above and in the synthesis of donor–acceptor complexes involving 2,2′-bipyridine and *closo*-stannacarboranes, described elsewhere,[7] 1.40 mmol (0.47 g) of I, 1.58 mmol (0.44 g), of II, or 0.34 mmol (0.09 g) of III was reacted with fresly sublimed, anhydrous 2,2′-bipyrimidine, $C_8H_6N_4$ (0.12 g, 1.14 mmol; 0.16 g, 1.01 mmol; or 0.04 g, 0.25 mmol; when I, II, or III was used) in dry benzene to isolate pure bright red, crystalline solid 1,1′-(2,2′-$C_8H_6N_4$)-[*closo*-1-Sn-2,3-($SiMe_3$)$_2$-2,3-$C_2B_4H_4$]$_2$ (VII) (0.42 g, 0.51 mmol; 73% yield based on I consumed), yellow-orange crystalline solid 1,1′-(2,2′-$C_8H_6N_4$)-[*closo*-1-Sn-2-($SiMe_3$)-3-(Me)-2,3-$C_2B_4H_4$]$_2$ (VIII) (0.40 g, 0.56 mmol; 71% yield based on II consumed), or red crystalline solid 1,1′-(2,2′-$C_8H_6N_4$)-[*closo*-1-Sn-2-($SiMe_3$)-2,3-$C_2B_4H_5$]$_2$ (IX) (0.08 g, 0.12 mmol; 71% yield based on III consumed) as the only sublimed reaction product on the inside walls of the detachable U-trap. In addition, a small quantity of unreacted 2,2′-bipyrimidine (0.06 g, 0.07 g, and a trace quantity when R = $SiMe_3$, Me, and H, respectively) was recovered in a trap held at −196 °C during the mild sublimation of the reaction residue. The stannacarboranes I, II, or III were not identified in the sublimate. Since the complexes VII, VIII, and IX are not soluble in *n*-hexane, they were washed with dry *n*-hexane in vacuo 2–3 times, vacuum dried, and then recrystallized in hot benzene.

The physical properties and characterization of VII are as follows: mp 170 °C dec; moderately stable in air for a brief period of time; at 25 °C, sparingly soluble in nonpolar organic solvents but slightly soluble in polar solvents, solubility increases at higher temperature without decomposition; ^1H NMR (353 K, C_6D_6, relative to external Me_4Si) δ 8.48 [d, 2 H, bpmd ring, $^3J(^1H-^1H)$ = 4.89 Hz], 6.36 [t, 1 H, bpmd ring, $^3J(^1H-^1H)$ = 4.88 Hz], 5.04 [q(br), 1 H, basal H_t, $^1J(^1H-^{11}B)$ = 141 Hz], 3.72 [q(br), 2 H, basal H_t, $^1J(^1H-^{11}B)$ = 145 Hz], 2.44 [q(br), 1 H, apical H_t, $^1J(^1H-^{11}B)$ = 158 Hz], 0.54 [s, 18 H, $SiMe_3$]; ^{11}B NMR (353 K, C_6D_6, relative to external $BF_3{\cdot}OEt_2$) δ 25.31 [d, 1 B, unique basal BH, $^1J(^{11}B-^1H)$ = 142 Hz], 22.92 [d, 2 B, basal BH, $^1J(^{11}B-^1H)$ = 145 Hz], −10.97 [d, 1 B, apical BH, $^1J(^{11}B-^1H)$ = 157 Hz]; ^{13}C NMR (363 K, C_6D_6, relative to external Me_4Si) δ 160.05 [s, bpmd ring, NCN], 156.71 [d, 2 CH, bpmd ring, $^1J(^{13}C-^1H)$ = 186 Hz], 132.93 [s(br), cage carbons (SiCB)], 121.92 [d, 1 CH, bpmd ring, $^1J(^{13}C-^1H)$ = 172 Hz], 2.69 [q(br), $SiMe_3$, $^1J(^{13}C-^1H)$ = 119 Hz]; ^{119}Sn NMR (363 K, C_6D_6, relative to external TMT) δ −174.27 [s(br), cage–Sn–bpmd]. Anal. Calcd for $C_{24}H_{50}B_8N_4Si_4Sn_2$: C, 34.69; H, 6.08; N, 6.74; B, 10.41; Si, 13.52; Sn, 28.57. Found: C, 33.78; H, 5.99; N, 6.81; B, 9.98; Si, 13.47; Sn, 28.83.

The physical properties and characterization of VIII are as follows: mp 162 °C dec; reasonably stable in air for a short period of time; at 25 °C, sparingly soluble in nonpolar organic solvents but slightly soluble in polar solvents, solubility increases at higher temperatures without decomposition; ^1H NMR (363 K, C_6D_6, relative to external Me_4Si) δ 8.45 [d, 2 H, bpmd ring, $^3J(^1H-^1H)$ = 4.88 Hz], 6.36 [t, 1 H, bpmd ring, $^3J(^1H-^1H)$ = 4.89 Hz], 4.96 [q(br), 1 H, basal H_t, $^1J(^1H-^{11}B)$ = 141 Hz], 3.76 [q(br), 2 H, basal H_t, $^1J(^1H-^{11}B)$ = 150 Hz], 2.67 [s(br), 3 H, C(cage)–Me], 2.43 [q(br), 1 H, apical H_t, $^1J(^1H-^{11}B)$ = 170 Hz], 0.29 [s, 9 H, $SiMe_3$]; ^{11}B NMR (363 K, C_6D_6, relative to external $BF_3{\cdot}OEt_2$) δ 23.05 [d, 1 B, unique basal BH, $^1J(^{11}B-^1H)$ = 141 Hz], 18.74 [d, 2 B, basal BH, $^1J(^{11}B-^1H)$ = 149 Hz], −8.88 [d, 1 B, apical BH, $^1J(^{11}B-^1H)$ = 169 Hz]; ^{13}C NMR (363 K, C_6D_6, relative to external Me_4Si) δ 161.0 [s, bpmd ring, NCN], 156.89 [d, 2 CH, bpmd ring, $^1J(^{13}C-^1H)$ = 185 Hz] 133.70 [s(br), cage carbon (SiCB)], 124.3 [s(br), cage carbon (CCB)], 121.63 [d, 1 CH, bpmd ring, $^1J(^{13}C-^1H)$ = 173 Hz], 23.39 [q, C(cage)–Me, $^1J(^{13}C-^1H)$ = 128 Hz], 1.26 [q, $SiMe_3$, $^1J(^{13}C-^1H)$ = 120 Hz]; ^{119}Sn NMR (363 K, C_6D_6, relative to external TMT) δ −125.80 [s(br), cage–Sn–bpmd]. Anal. Calcd for $C_{20}H_{38}B_8N_4Si_2Sn_2$: C, 33.62; H, 5.36; N, 7.84; Sn, 33.22. Found: C, 33.59; H, 5.44; N, 7.81; Sn, 32.88.

The physical properties and characterization of IX are as follows: mp 159–161 °C dec; moderately stable in air for a brief period of time; at 25 °C, sparingly soluble in nonpolar organic solvents but slightly soluble in polar solvents, solubility increases at higher temperatures without decomposition; ^1H NMR (363 K, C_6D_6, relative to external Me_4Si) δ 8.47 [d, 2 H, bpmd ring, $^3J(^1H-^1H)$ = 4.89 Hz], 7.19 [s(br), 1 H, cage CH], 6.36 [t, 1 H, bpmd ring, $^3J(^1H-^1H)$ = 4.88 Hz], 5.05 [q(br), 1 H, basal H_t, $^1J(^1H-^{11}B)$ = 135 Hz], 3.79 [q(br), 2 H, basal H_t, $^1J(^1H-^{11}B)$ = 151 Hz], 2.53 [q(br), 1 H, apical H_t, $^1J(^1H-^{11}B)$ = 171 Hz], 0.54 [s, 9 H, $SiMe_3$]; ^{11}B NMR (363 K, C_6D_6, relative to external $BF_3{\cdot}OEt_2$) δ 23.40 [d, 1 B, unique basal BH, $^1J(^{11}B-^1H)$ = 134 Hz], 16.55 [d, 2 B, basal BH, $^1J(^{11}B-^1H)$ = 152 Hz], −17.25 [d, 1 B, apical BH, $^1J(^{11}B-^1H)$ = 172 Hz]; ^{13}C NMR (363 K, C_6D_6, relative to external Me_4Si) δ 160.44 [s, bpmd ring, NCN], 157.0 [d, 2 CH, bpmd ring, $^1J(^{13}C-^1H)$ = 185.3 Hz], 132.9 [s(br), cage carbon (SiCB)], 121.68 [d, 1 CH, bpmd ring, $^1J(^{13}C-^1H)$ = 170 Hz], 118.13 [d(br), cage CH, $^1J(^{13}C-^1H)$ = 177 Hz], 0.10 [q, $SiMe_3$, $^1J(^{13}C-^1H)$ = 119.6 Hz]; ^{119}Sn NMR (363 K, C_6D_6, relative to external TMT) δ −135.01 [s(br), cage–Sn–bpmd]. Anal. Calcd for $C_{18}H_{34}B_8N_4Si_2Sn_2$: C, 31.49; H, 4.99; N, 8.16; Sn, 34.58. Found: C, 31.51; H, 4.95; N, 8.15; Sn, 34.48.

Calculations. Semiempirical MNDO-SCF calculations were carried out by using Version[14] 2.10 of the MOPAC package[15] on an IBM 3081 running under the VM/CMS operating system. The parameters for the elements involved are those determined by Dewar and co-workers.[16-18]

X-ray Analyses of *closo*-1-Sn[(η^5-C_5H_5)Fe(η^5-$C_5H_4CH_2$-$(Me)_2N$)]-2,3-($SiMe_3$)$_2$-2,3-$C_2B_4H_4$ (IV) and 1,1′-(2,2′-$C_8H_6N_4$)-[*closo*-1-Sn-2,3-($SiMe_3$)$_2$-2,3-$C_2B_4H_4$]$_2$ (VII). Yellow-orange crystals of IV were grown very slowly in C_6H_6 solution. Since the crystals of IV changed to opaque white upon brief exposure to air, they were coated with an epoxy resin. Data were collected at 299 K, using an automatic Nicolet R3m/V diffractometer approximately along the *a* axis. Red-orange crystals of VII were grown by vacuum sublimation onto a glass surface. Suitable crystals of VII were sealed in 0.7-mm capillary tubes under dry argon. The data collection for VII was carried out at 163 K by using an upgraded Nicolet P1 to P3F diffractometer approximately along the *a* axis. Unit-cell dimensions were refined by least-squares fit of 25 reflections measured in the range $15 < 2\theta < 25°$ for both IV and VII. The pertinent crystallographic data are summarized in Table I. Three standard reflections were measured after every 100 reflections during the data collections. Data were corrected for decay and Lorentz–polarization effects. An absorption correction was applied for IV based on ψ scans but no absorption correction for VII. The structures were solved by direct methods using SHELXTL-Plus[19] and subsequent difference Fourier maps. All hydrogen atoms were placed in calculated positions with fixed isotropic temperature factors. Final full-matrix least-squares refinements of non-hydrogen atoms with anisotropic temperature factors were carried out by using SHELXTL-Plus. The function minimized being $\sum w(|F_o| - |F_c|)^2$. In the final stages of refinement a weighting scheme was used (Table I). Scattering factors and real and imaginary parts of anomalous dispersion corrections for Sn and Si used were those stored in SHELXTL-Plus. The final atomic coordinates for IV and VII are given in Table II. Selected bond lengths, bond angles,

(14) Olivella, S. *QCPE Bull.* **1984**, *4*, 109.
(15) Stewart, J. J. P. *QCPE Bull.* **1983**, *3*, 43.
(16) Dewar, M. J. S.; Thiel, W. *J. Am. Chem. Soc.* **1977**, *99*, 4899.
(17) Dewar, M. J. S.; McKee, M. L. *J. Am. Chem. Soc.* **1977**, *99*, 5231.
(18) Dewar, M. J. S.; Holloway, M. K.; Grady, G. L.; Stewart, J. J. P. *Organometallics* **1985**, *4*, 1973.
(19) Sheldrick, G. M. *Structure Determination Software Programs*; Nicolet Instrument Corp., USA, 1988.

Table I. Crystallographic Data[a] for IV and VII

	IV	VII
formula	$C_{21}H_{39}B_4NSi_2FeSn$	$C_{24}H_{50}B_8N_4Si_4Sn_2$
fw	579.24	831.00
cryst system	triclinic	monoclinic
space group	$P\bar{1}$	$P2_1/c$
a, Å	12.710 (3)	15.884 (4)
b, Å	14.329 (5)	9.841 (3)
c, Å	17.443 (6)	13.550 (4)
α, deg	102.59 (3)	
β, deg	97.48 (3)	104.71 (2)
γ, deg	110.00 (3)	
U, Å^3	2839.9 (15)	2048.4 (9)
Z	4	2
D_{calcd}, g cm^{-3}	1.36	1.35
cryst dimens, mm	0.5 × 0.4 × 0.2	0.3 × 0.4 × 0.1
μ(Mo Kα), cm^{-1}	14.85	13.57
scan type	$\theta/2\theta$	$\theta/2\theta$
scan speed in ω (min, max)	3.0, 15.0	4.00, 15.00
2θ range	3.0–45.0	3.0–45.0
data collected	$\pm h,\pm k,l$	$\pm h,k,l$
T, K	299	163
decay, %	18	10
unique data	7447	4676
obsd reflctns, $F > 6.0\sigma(F)$	6103	3481
R[b]	0.060	0.059
R_w	0.068	0.076
$\Delta\rho$(max,min), e/Å^3	1.28 (close to Sn), −1.08	0.81, −0.9
k[c]	0.0066	0.0137

[a] Graphite-monochromatized Mo Kα radiation, λ = 0.71073 Å. [b] $R = \sum||F_o| - |F_c||/\sum|F_o|$ and $R_w = [\sum\omega(F_o - F_c)^2/\sum(F_o)^2]^{1/2}$. [c] $\omega = 1/[\sigma^2(F_o) + k(F_o)^2]$.

and torsion angles are presented in Table III.

Results and Discussion

Synthesis. In our earlier work we have shown that the *closo*-stannacarboranes react almost instantaneously with 2,2′-bipyridine in benzene to form donor–acceptor complexes in high yield.[7] In the present study, the stannacarboranes I–III react with the bis(bidentate) ligand 2,2′-bipyrimidine almost immediately to form the corresponding bridged donor–acceptor complexes VII–IX in 71–73% yields (see Scheme I). However, the reaction with (ferrocenylmethyl)-*N*,*N*-dimethylamine was somewhat slower. Complexes IV–VI were produced in yields ranging from 61 to 80%. When either of the reagents was taken in large excess, there was no change in the formation and yields of the products, and the excess reagent was recovered unchanged. Unlike during the formation of donor–acceptor complexes of germacarboranes[20] there was no indication of any kinetically controlled processes to produce adducts between I–III and the Lewis bases. Since the complexes IV–IX are all colored from yellow-orange to bright red, there may be some degree of charge transfer due to $\eta \rightarrow \pi^*$ transitions as in the bipyridine complexes of *closo*-germacarboranes.[20] The donor–acceptor complexes IV–VI are all highly soluble in benzene whereas the bridged complexes VII–IX are only sparingly soluble in that solvent. In fact, the NMR tube containing the heterogeneous mixture of this complex and the solvent C_6D_6 had to be heated around 353–363 K before the spectra were run. Apparently, the presence of a ferrocenyl moiety results in the greater solubility of complexes IV–VI in benzene and in other nonpolar and polar organic solvents. Most of these donor–acceptor complexes do not melt to form a clear solution but instead decompose above 413 K to form a reddish brown polymeric mass in addition to release of the starting materials in measurable quantities. This indicates that the Sn–N bonds in these complexes are weak.

Characterization. The donor–acceptor complexes IV, V, VI, VII, VIII, and IX were characterized on the basis of ^{1}H, ^{11}B, ^{13}C, and ^{119}Sn pulse Fourier transform NMR and IR and where possible by mass spectroscopy and elemental analysis (Experimental Section and supplementary Tables I and II). Complexes IV and VII were also characterized by single-crystal X-ray diffraction (Tables I–III).

Mass Spectra. The electron-impact (EI) mass spectra of IV, VII, and IX (supplementary Table I) do not exhibit the parent ion groupings. In each spectrum, the Lewis base ion fragment [$(C_5H_5)Fe(C_5H_4CH_2(CH_3)_2N)$ for IV and $C_8H_6N_4$ for VII and IX] with 100% relative intensity, and the parent and the daughter (parent minus a methyl unit) groupings of the corresponding stannacarborane precursor have been observed. This indicates that the Sn–N bonds in the complexes are weak; consequently, these bonds were broken during the ionization at 70 eV.

NMR and IR Spectra. The ^{1}H NMR and ^{13}C NMR spectra clearly indicate the presence of (ferrocenylmethyl)-*N*,*N*-dimethylamine ligand in IV–VI and a 2,2′-bipyrimidine molecule in VII–IX in addition to the $SiMe_3$ and Me or CH groups, respectively. There is no significant change in the ^{13}C chemical shift of the cage carbons from those of the stannacarborane precursors, indicating that the extent of the interaction of the apical tin with the cage carbons remained more or less the same even after the formation of coordinate covalent bond(s) between the tin and the N-donor atom(s). This was also the case for the corresponding 2,2′-bipyridine complexes,[7] indicating that ^{13}C chemical shift is not a sensitive probe for the study of structural distortions in this system. Among all the spectroscopic data, the ^{11}B and ^{119}Sn NMR spectra provide the most significant and interesting information regarding the geometries of the donor–acceptor complexes IV–IX. The ^{11}B NMR spectra of all the complexes exhibit a clear separation of the unique BH resonance from the remaining two basal BH resonances (see Experimental Section). A significant upfield shift of the apical BH resonance is consistent with the interpretation that the interaction of the apical BH with the tin atom, transmitted through the basal atoms, is significantly weaker than that of the stannacarborane precursor as the same π-type orbitals of the tin that were originally interacting with the apical BH are now utilized, at least in part, to accommodate the lone pair of electrons on the nitrogen atom(s) of the ligand. A clear splitting of the basal BH resonances is consistent with the slippage of the tin toward the unique boron above the C_2B_3 face, and this has been observed previously.[7] It is important to point out that the splitting of the basal BH resonances in the ^{11}B NMR spectra of most of the known symmetrical, neutral compounds of the C_2B_4 system is not a common occurrence.[5] The ^{119}Sn NMR chemical shifts of all the donor–acceptor complexes of the stannacarboranes with N-donor atoms are shifted downfield from those of the corresponding stannacarborane precursors (complexes VII, VIII, and IX by 30–80 ppm; IV, V, and VI by 125–180 ppm; and the 2,2′-bipyridine analogues by 63–101 ppm).[7] The ^{119}Sn NMR spectra of the THF complexes 1-Sn(THF)$_2$-2-($SiMe_3$)-3-(R)-2,3-$C_2B_4H_4$ (R = $SiMe_3$, Me, H) show upfield shifts of 9, 28, and 13 ppm, respectively.[7] These results indicate that the relationship between the ^{119}Sn chemical shift and complex formation is a complex one and cannot be explained on simple

(20) Hosmane, N. S.; Islam, M. S.; Pinkston, B. S.; Siriwardane, U.; Banewicz, J. J.; Maguire, J. A. *Organometallics* **1988**, *7*, 2340.

Table II. Atomic Coordinates (×10⁴) and Equivalent Isotropic Displacement Coefficients (Å² × 10³) for IV and VII

	x	y	z	U(eq)		x	y	z	U(eq)
				IV					
Sn(1)	-3408 (1)	2411 (1)	-2642 (1)	51 (1)	Sn(2)	1606 (1)	2092 (1)	2214 (1)	50 (1)
Fe(1)	-2540 (1)	2191 (1)	355 (1)	51 (1)	Fe(2)	2371 (1)	1980 (1)	5141 (1)	52 (1)
Si(1)	-2831 (2)	2785 (2)	-4883 (1)	61 (1)	Si(3)	2472 (2)	3411 (2)	405 (1)	64 (1)
Si(2)	-272 (2)	4160 (2)	-3021 (2)	79 (1)	Si(4)	4861 (2)	4026 (2)	2299 (1)	70 (1)
N(1)	-4819 (5)	1127 (5)	-2083 (4)	61 (3)	N(2)	195 (5)	597 (5)	2649 (4)	63 (3)
C(11)	-2553 (6)	2414 (5)	-3939 (4)	48 (3)	C(21)	2641 (6)	2596 (5)	1079 (4)	48 (3)
C(12)	-1539 (6)	2931 (6)	-3246 (4)	54 (3)	C(22)	3558 (6)	2838 (6)	1793 (4)	49 (3)
B(13)	-1537 (9)	2270 (9)	-2625 (7)	92 (5)	B(23)	3411 (8)	1848 (9)	2110 (7)	68 (5)
B(14)	-2684 (8)	1101 (7)	-3084 (7)	65 (4)	B(24)	2298 (9)	880 (7)	1461 (7)	63 (4)
B(15)	-3347 (7)	1314 (7)	-3906 (6)	58 (4)	B(25)	1779 (8)	1434 (7)	839 (6)	59 (4)
B(16)	-1846 (8)	1640 (7)	-3708 (6)	58 (4)	B(26)	3273 (8)	1700 (7)	1070 (6)	61 (4)
C(13)	609 (17)	4428 (16)	-2154 (13)	465 (29)	C(23)	5945 (11)	3726 (13)	2834 (12)	195 (12)
C(14)	-636 (13)	5215 (10)	-2955 (17)	429 (27)	C(24)	4451 (12)	4868 (9)	3053 (10)	181 (9)
C(15)	578 (14)	4171 (15)	-3727 (14)	344 (21)	C(25)	5590 (11)	4694 (13)	1653 (8)	219 (12)
C(16)	-2863 (17)	4031 (10)	-4698 (9)	243 (14)	C(26)	984 (8)	2913 (11)	-175 (8)	124 (8)
C(17)	-4284 (9)	1962 (11)	-5478 (7)	125 (8)	C(27)	2714 (16)	4725 (10)	1004 (8)	205 (13)
C(18)	-1845 (13)	2612 (18)	-5533 (9)	271 (23)	C(28)	3408 (11)	3451 (13)	-299 (8)	142 (10)
C(19)	-5434 (7)	103 (8)	-2676 (6)	85 (5)	C(29)	-257 (8)	-417 (7)	2069 (5)	85 (4)
C(110)	-5624 (7)	1604 (8)	-1892 (5)	80 (5)	C(210)	-744 (6)	947 (8)	2762 (6)	80 (5)
C(111)	-4227 (7)	975 (7)	-1344 (5)	65 (4)	C(211)	781 (6)	554 (6)	3423 (5)	60 (4)
C(112)	-3433 (6)	1996 (6)	-758 (4)	57 (3)	C(213)	2759 (6)	2046 (7)	4062 (5)	62 (4)
C(113)	-2229 (6)	2445 (7)	-707 (5)	60 (4)	C(214)	3182 (8)	3050 (8)	4587 (6)	83 (5)
C(114)	-1778 (7)	3385 (7)	-94 (5)	67 (4)	C(212)	1540 (6)	1596 (6)	3963 (4)	52 (3)
C(115)	-2667 (7)	3524 (7)	236 (6)	73 (4)	C(215)	2260 (9)	3243 (7)	4838 (6)	89 (5)
C(116)	-3686 (7)	2679 (7)	-177 (5)	67 (4)	C(216)	1250 (7)	2365 (7)	4466 (5)	64 (4)
C(117)	-2994 (10)	793 (7)	559 (6)	82 (5)	C(217)	1835 (9)	695 (7)	5527 (5)	75 (4)
C(118)	-3233 (10)	1483 (7)	1161 (6)	84 (5)	C(218)	1654 (9)	1520 (7)	6043 (5)	78 (5)
C(119)	-2201 (8)	2306 (7)	1551 (5)	73 (4)	C(219)	2741 (9)	2323 (8)	6361 (5)	81 (5)
C(120)	-1315 (9)	2152 (7)	1215 (5)	75 (4)	C(220)	3564 (8)	2023 (8)	6057 (6)	78 (5)
C(121)	-1813 (10)	1195 (8)	590 (5)	80 (5)	C(221)	2998 (9)	1006 (8)	5538 (5)	79 (5)
				VII					
Sn	6595 (1)	1254 (1)	4009 (1)	50 (1)	C(3)	8745 (12)	3930 (6)	3904 (5)	128 (2)
Si(1)	7857 (2)	4078 (2)	2735 (2)	68 (1)	C(4)	8288 (12)	4553 (17)	1712 (10)	179 (1)
Si(2)	8579 (2)	287 (4)	2626 (3)	98 (1)	C(5)	7199 (13)	5440 (14)	2967 (21)	38 (3)
N(1)	5817 (4)	-888 (6)	4547 (4)	49 (1)	C(6)	9337 (13)	1388 (14)	2194 (20)	27 (3)
N(2)	4890 (4)	-1616 (6)	5569 (5)	48 (1)	C(7)	9003 (14)	-475 (24)	3750 (12)	25 (2)
C(1)	7209 (4)	2473 (7)	2602 (5)	44 (1)	C(8)	8416 (11)	-1070 (14)	1609 (14)	161 (7)
C(2)	7510 (5)	1043 (7)	2628 (6)	49 (1)	C(9)	5194 (4)	-717 (7)	5035 (5)	42 (1)
B(3)	6716 (6)	2 (8)	2500 (6)	49 (2)	C(10)	6157 (5)	-2134 (8)	4598 (6)	62 (2)
B(4)	5817 (5)	980 (8)	2272 (6)	47 (2)	C(11)	5877 (6)	-3158 (8)	5131 (7)	67 (2)
B(5)	6189 (5)	2595 (8)	2419 (6)	48 (2)	C(12)	5249 (5)	-2859 (7)	5627 (6)	58 (2)
B(6)	6608 (5)	1434 (8)	1647 (6)	48 (2)					

[a] Equivalent isotropic U defined as one-third of the trace of the orthogonalized U_{ij} tensor.

charge-density arguments. Theoretical studies are now underway to attempt to explain the differences in the observed ^{119}Sn NMR chemical shifts in these donor–acceptor complexes. Preliminary results of the Fenske–Hall type of MO calculations[21] on IV–VI indicate that the apical tin atom of the stannacarborane cage is interacting not only with the sp³-hybridized nitrogen atom of the Lewis base but also with the lower substituted cyclopentadienyl ring of the ferrocene fragment so as to form a triple-decker sandwich complex of the type $(\eta^5\text{-}C_5H_5)Fe(\eta^5\text{-}C_5H_4CH_2\text{-}(CH_3)_2N)Sn(R_2C_2B_4H_4)$. It may be that it is this additional π-interaction that causes the ^{119}Sn resonances in the donor–acceptor complexes IV, V, and VI to shift downfield significantly (see Experimental Section). The presence of the stannacarborane cages and the corresponding Lewis bases were also confirmed by the infrared (IR) spectra of IV–IX (see supplementary Table II).

Crystal Structures of *closo*-1-Sn[$(\eta^5$-$C_5H_5)Fe(\eta^5$-$C_5H_4CH_2(Me)_2N)$]-2,3-$(SiMe_3)_2$-2,3-$C_2B_4H_4$ (IV) and 1,1′-(2,2′-$C_8H_6N_4$)-[*closo*-1-Sn-2,3-$(SiMe_3)_2$-2,3-$C_2B_4H_4$]$_2$ (VII) and MNDO–SCF Calculations on VII. The X-ray crystal structure of IV reveals that the unit cell consists of two crystallographically independent molecules. Figure 1 shows the thermal ellipsoids of one of the molecules (molecule 1), and Figure 2 is a superimposed line drawing of the two structures. Table IV summarizes some structural parameters that allow a comparison of the two molecules. As can be seen from this table, in molecule 2 the Sn–N bond is almost directly over the unique boron [B(4)] while in molecule 1 it is slightly rotated away from this boron. Molecule 2 also has a longer Sn–N bond distance, has a greater tilt of the ferrocenylalkylamine base (as measured by the N–Sn–B(4)) bond angles, and is less slip distorted, as measured by the differences in the Δ's, than is molecule 1 (see Table IV). Analysis of other stannacarborane–base systems (vide infra) has shown that an increased slip distortion and a decreased tilt angle should accompany increased tin–base interactions.[22] This is what is found for the two structures compared in Table IV. The slip distortions exhibited by both of these compounds, as measured by the differences in the Sn–C(cage) and Sn–B(unique) bond distances [0.26 and 0.20 Å for molecules 1 and 2, respectively], are considerably less than those observed in 1-Sn($C_{10}H_8N_2$)-2,3-$(SiMe_3)_2$-2,3-$C_2B_4H_4$ (0.38 Å),[7] 1-Sn($C_{10}H_8N_2$)-2-$(SiMe_3)$-3-Me-2,3-$C_2B_4H_4$ (0.46 Å),[8] and 1-Sn($C_{10}H_8N_2$)-2,3-$(Me)_2$-2,3-$C_2B_9H_9$ (0.52 Å)[9,10]

(21) Barreto, R. D.; Maguire, J. A.; Hosmane, N. S.; Fehlner, T. P., to be submitted for publication.

(22) Maguire, J. A.; Ford, G. P.; Hosmane, N. S. *Inorg. Chem.* **1988**, *27*, 3354.

Table III. Bond Lengths (Å), Bond Angles (deg), and Torsion Angles (deg) for IV and VII

Bond Lengths for IV

A. Molecule 1

Sn(1)–N(1)	2.557 (7)	Sn(1)–C(11)	2.635 (8)	C(11)–B(16)	1.727 (15)	C(12)–B(13)	1.586 (16)
Sn(1)–C(12)	2.664 (8)	Sn(1)–B(13)	2.451 (12)	C(12)–B(16)	1.732 (12)	B(13)–B(14)	1.737 (12)
Sn(1)–B(14)	2.388 (12)	Sn(1)–B(15)	2.439 (10)	B(13)–B(16)	1.832 (14)	B(14)–B(15)	1.705 (16)
Sn(1)–C(112)	3.468 (10)	Sn(1)–C(113)	3.492 (8)	B(14)–B(16)	1.739 (16)	B(15)–B(16)	1.768 (13)
Sn(1)–C(114)	4.348 (9)	Sn(1)–C(115)	4.783 (10)	Fe(1)–C(112)	2.026 (8)	Fe(1)–C(113)	2.028 (9)
Sn(1)–C(116)	4.305 (8)	Si(1)–C(11)	1.865 (8)	Fe(1)–C(114)	2.032 (9)	Fe(1)–C(115)	2.023 (11)
Si(2)–C(12)	1.856 (7)	N(1)–C(19)	1.475 (10)	Fe(1)–C(116)	2.024 (10)	Fe(1)–C(117)	2.011 (10)
N(1)–C(110)	1.447 (13)	N(1)–C(111)	1.502 (12)	Fe(1)–C(118)	2.028 (11)	Fe(1)–C(119)	2.032 (9)
C(11)–C(12)	1.490 (9)	C(11)–B(15)	1.574 (11)	Fe(1)–C(120)	2.039 (11)	Fe(1)–C(121)	2.028 (14)

B. Molecule 2

Sn(1)–N(2)	2.613 (9)	Sn(2)–C(21)	2.613 (8)	C(21)–B(26)	1.730 (15)	C(22)–B(23)	1.593 (16)
Sn(2)–C(22)	2.616 (7)	Sn(2)–B(23)	2.460 (12)	C(22)–B(26)	1.720 (12)	B(23)–B(24)	1.662 (12)
Sn(2)–B(24)	2.422 (12)	Sn(2)–B(25)	2.446 (10)	B(23)–B(26)	1.757 (16)	B(24)–B(25)	1.670 (17)
Sn(2)–C(212)	3.286 (9)	Sn(2)–C(213)	3.387 (8)	B(24)–B(26)	1.719 (15)	B(25)–B(26)	1.775 (14)
Sn(2)–C(214)	4.063 (10)	Sn(2)–C(215)	4.375 (8)	Fe(2)–C(213)	2.021 (9)	Fe(2)–C(214)	2.043 (11)
Sn(2)–C(216)	3.964 (8)	Si(3)–C(21)	1.871 (9)	Fe(2)–C(212)	2.045 (7)	Fe(2)–C(215)	2.037 (12)
Si(4)–C(22)	1.859 (6)	N(2)–C(29)	1.449 (10)	Fe(2)–C(216)	2.024 (10)	Fe(2)–C(217)	2.027 (10)
N(2)–C(210)	1.464 (13)	N(2)–C(211)	1.478 (11)	Fe(2)–C(218)	2.039 (10)	Fe(2)–C(219)	2.029 (8)
C(21)–C(22)	1.478 (10)	C(21)–B(25)	1.573 (11)	Fe(2)–C(220)	2.029 (11)	Fe(2)–C(221)	2.025 (13)

Bond Angles for IV

A. Molecule 1

N(1)–Sn(1)–C(11)	138.6 (2)	N(1)–Sn(1)–C(12)	149.0 (3)	C(11)–C(12)–B(13)	112.9 (6)	Sn(1)–C(12)–B(16)	90.6 (4)
C(11)–Sn(1)–C(12)	32.7 (2)	N(1)–Sn(1)–B(13)	115.9 (4)	Si(2)–C(12)–B(16)	135.5 (6)	C(11)–C(12)–B(16)	64.3 (5)
C(11)–Sn(1)–B(13)	60.4 (3)	C(12)–Sn(1)–B(13)	35.8 (4)	B(13)–C(12)–B(16)	66.8 (6)	Sn(1)–B(13)–C(12)	79.4 (6)
N(1)–Sn(1)–B(14)	87.5 (3)	C(11)–Sn(1)–B(14)	62.7 (3)	Sn(1)–B(13)–B(14)	67.0 (5)	C(12)–B(13)–B(14)	104.4 (7)
C(12)–Sn(1)–B(14)	62.4 (3)	B(13)–Sn(1)–B(14)	42.0 (3)	Sn(1)–B(13)–B(16)	95.3 (5)	C(12)–B(13)–B(16)	60.4 (6)
N(1)–Sn(1)–B(15)	102.9 (3)	C(11)–Sn(1)–B(15)	35.9 (3)	B(14)–B(13)–B(16)	58.3 (6)	Sn(1)–B(14)–B(13)	70.9 (6)
C(12)–Sn(1)–B(15)	59.7 (2)	B(13)–Sn(1)–B(15)	67.2 (3)	Sn(1)–B(14)–B(15)	70.9 (5)	B(13)–B(14)–B(15)	103.7 (8)
B(14)–Sn(1)–B(15)	41.3 (4)	Sn(1)–N(1)–C(19)	112.7 (5)	Sn(1)–B(14)–B(16)	100.1 (6)	B(13)–B(14)–B(16)	63.6 (6)
Sn(1)–N(1)–C(110)	103.7 (6)	C(19)–N(1)–C(110)	109.8 (6)	B(15)–B(14)–B(16)	61.8 (6)	Sn(1)–B(15)–C(11)	78.9 (4)
Sn(1)–N(1)–C(111)	111.7 (4)	C(19)–N(1)–C(111)	108.0 (7)	Sn(1)–B(15)–B(14)	67.7 (5)	C(11)–B(15)–B(14)	106.1 (6)
C(110)–N(1)–C(111)	111.0 (7)	Sn(1)–C(11)–Si(1)	136.1 (4)	Sn(1)–B(15)–B(16)	97.4 (4)	C(11)–B(15)–B(16)	61.9 (6)
Sn(1)–C(11)–C(12)	74.7 (4)	Si(1)–C(11)–C(12)	128.7 (5)	B(14)–B(15)–B(16)	60.1 (6)	C(11)–B(16)–C(12)	51.0 (5)
Sn(1)–C(11)–B(15)	65.3 (4)	Si(1)–C(11)–B(15)	117.9 (5)	C(11)–B(16)–B(13)	92.1 (7)	C(12)–B(16)–B(13)	52.8 (6)
C(12)–C(11)–B(15)	112.4 (7)	Sn(1)–C(11)–B(16)	91.7 (5)	C(11)–B(16)–B(14)	98.3 (7)	C(12)–B(16)–B(14)	98.4 (7)
Si(1)–C(11)–B(16)	130.7 (6)	C(12)–C(11)–B(16)	64.7 (5)	B(13)–B(16)–B(14)	58.1 (5)	C(11)–B(16)–B(15)	53.5 (5)
B(15)–C(11)–B(16)	64.6 (6)	Sn(1)–C(12)–Si(2)	132.3 (4)	C(12)–B(16)–B(15)	93.3 (7)	B(13)–B(16)–B(15)	97.5 (7)
Sn(1)–C(12)–C(11)	72.6 (4)	Si(2)–C(12)–C(11)	131.3 (6)	B(14)–B(16)–B(15)	58.2 (6)	N(1)–C(111)–C(112)	111.3 (8)
Sn(1)–C(12)–B(13)	64.8 (5)	Si(2)–C(12)–B(13)	115.8 (5)				

B. Molecule 2

N(2)–Sn(2)–C(21)	145.8 (3)	N(2)–Sn(2)–C(22)	147.5 (3)	C(21)–C(22)–B(23)	111.3 (6)	Sn(2)–C(22)–B(26)	92.6 (4)
C(21)–Sn(2)–C(22)	32.8 (2)	N(2)–Sn(2)–B(23)	111.3 (3)	Si(4)–C(22)–B(26)	134.9 (6)	C(21)–C(22)–B(26)	65.0 (5)
C(21)–Sn(2)–B(23)	59.9 (4)	C(22)–Sn(2)–B(23)	36.4 (4)	B(23)–C(22)–B(26)	63.9 (6)	Sn(2)–B(23)–C(22)	77.1 (6)
N(2)–Sn(2)–B(24)	89.9 (4)	C(21)–Sn(2)–B(24)	61.9 (3)	Sn(2)–B(23)–B(24)	68.9 (6)	C(22)–B(23)–B(24)	105.9 (8)
C(22)–Sn(2)–B(24)	61.9 (3)	B(23)–Sn(2)–B(24)	39.8 (3)	Sn(2)–B(23)–B(26)	97.2 (6)	C(22)–B(23)–B(26)	61.6 (6)
N(2)–Sn(2)–B(25)	109.8 (4)	C(21)–Sn(2)–B(25)	36.1 (2)	B(24)–B(23)–B(26)	60.3 (6)	Sn(2)–B(24)–B(23)	71.3 (6)
C(22)–Sn(2)–B(25)	59.7 (2)	B(23)–Sn(2)–B(25)	65.0 (4)	Sn(2)–B(24)–B(25)	70.7 (5)	B(23)–B(24)–B(25)	104.6 (8)
B(24)–Sn(2)–B(25)	40.1 (4)	Sn(2)–N(2)–C(29)	115.9 (5)	Sn(2)–B(24)–B(26)	99.6 (6)	B(23)–B(24)–B(26)	62.6 (6)
Sn(2)–N(2)–C(210)	102.4 (6)	C(29)–N(2)–C(210)	109.4 (6)	B(25)–B(24)–B(26)	63.1 (6)	Sn(2)–B(25)–C(21)	77.8 (4)
Sn(2)–N(2)–C(211)	108.3 (5)	C(29)–N(2)–C(211)	110.0 (7)	Sn(2)–B(25)–B(24)	69.2 (5)	C(21)–B(25)–B(24)	106.3 (6)
C(210)–N(2)–C(211)	110.5 (7)	Sn(2)–C(21)–Si(3)	131.7 (4)	Sn(2)–B(25)–B(26)	97.2 (5)	C(21)–B(25)–B(26)	61.9 (5)
Sn(2)–C(21)–C(22)	73.7 (4)	Si(3)–C(21)–C(22)	129.6 (5)	B(24)–B(25)–B(26)	59.8 (6)	C(21)–B(26)–C(22)	50.7 (5)
Sn(2)–C(21)–B(25)	66.2 (4)	Si(3)–C(21)–B(25)	118.5 (5)	C(21)–B(26)–B(23)	93.3 (7)	C(22)–B(26)–B(23)	54.5 (6)
C(22)–C(21)–B(25)	111.6 (7)	Sn(2)–C(21)–B(26)	92.5 (5)	C(21)–B(26)–B(24)	97.6 (7)	C(22)–B(26)–B(24)	98.1 (7)
Si(3)–C(21)–B(26)	134.6 (6)	C(22)–C(21)–B(26)	64.3 (5)	B(23)–B(26)–B(24)	57.1 (6)	C(21)–B(26)–B(25)	53.3 (5)
B(25)–C(21)–B(26)	64.8 (6)	Sn(2)–C(22)–Si(4)	130.7 (4)	C(22)–B(26)–B(25)	92.5 (7)	B(23)–B(26)–B(25)	96.6 (7)
Sn(2)–C(22)–C(21)	73.5 (4)	Si(4)–C(22)–C(21)	131.2 (6)	B(24)–B(26)–B(25)	57.1 (6)	N(2)–C(211)–C(212)	112.8 (7)
Sn(2)–C(22)–B(23)	66.5 (5)	Si(4)–C(22)–B(23)	117.2 (5)				

Torsion Angles for IV

A. Molecule 1

C(11)–Sn(1)–N(1)–C(19)	−7.7 (8)	C(11)–Sn(1)–N(1)–C(110)	126.4 (5)
C(11)–Sn(1)–N(1)–C(111)	114.1 (5)	C(12)–Sn(1)–N(1)–C(19)	−62.0 (7)
C(12)–Sn(1)–N(1)–C(110)	179.3 (4)	C(12)–Sn(1)–N(1)–C(111)	59.8 (7)
B(13)–Sn(1)–N(1)–C(19)	−81.5 (7)	B(13)–Sn(1)–N(1)–C(110)	159.9 (5)
B(13)–Sn(1)–N(1)–C(111)	40.3 (6)	B(14)–Sn(1)–N(1)–C(19)	−49.5 (7)
B(14)–Sn(1)–N(1)–C(110)	−168.1 (5)	B(14)–Sn(1)–N(1)–C(111)	72.3 (6)
B(15)–Sn(1)–N(1)–C(19)	−10.8 (7)	B(15)–Sn(1)–N(1)–C(110)	−129.5 (5)
B(15)–Sn(1)–N(1)–C(111)	111.0 (6)	N(1)–Sn(1)–C(11)–Si(1)	100.1 (5)
N(1)–Sn(1)–C(11)–C(12)	−129.3 (5)	N(1)–Sn(1)–C(11)–B(15)	−5.2 (7)
N(1)–Sn(1)–C(11)–B(16)	−66.1 (5)	N(1)–Sn(1)–C(12)–Si(2)	−133.6 (5)
N(1)–Sn(1)–C(12)–C(11)	95.9 (6)	N(1)–Sn(1)–C(12)–B(13)	−30.8 (6)
N(1)–Sn(1)–C(12)–B(16)	33.1 (6)	N(1)–Sn(1)–B(13)–C(12)	163.0 (4)
N(1)–Sn(1)–B(13)–B(14)	52.3 (6)	N(1)–Sn(1)–B(13)–B(16)	104.4 (6)
N(1)–Sn(1)–B(14)–B(13)	−134.6 (6)	N(1)–Sn(1)–B(14)–B(15)	112.8 (4)
N(1)–Sn(1)–B(14)–B(16)	168.1 (5)	N(1)–Sn(1)–B(15)–C(11)	176.5 (4)
N(1)–Sn(1)–B(15)–B(14)	−70.8 (4)	N(1)–Sn(1)–B(15)–B(16)	−124.2 (5)
Sn(1)–N(1)–C(111)–C(112)	46.9 (8)	C(19)–N(1)–C(111)–C(112)	171.4 (7)
C(110)–N(1)–C(111)–C(112)	−68.3 (8)	N(1)–C(111)–C(112)–Fe(1)	175.3 (6)
N(1)–C(111)–C(112)–C(113)	−97 (1)	N(1)–C(111)–C(112)–C(116)	83 (1)

Table III (Continued)

Torsion Angles for IV

B. Molecule 2

C(21)-Sn(2)-N(2)-C(29)	0.4 (8)	C(21)-Sn(2)-N(2)-C(210)	-118.6 (6)
C(21)-Sn(2)-N(2)-C(211)	124.6 (5)	C(22)-Sn(2)-N(2)-C(29)	-61.4 (8)
C(22)-Sn(2)-N(2)-C(210)	179.6 (4)	C(22)-Sn(2)-N(2)-C(211)	62.8 (8)
B(23)-Sn(2)-N(2)-C(29)	-67.1 (8)	B(23)-Sn(2)-N(2)-C(210)	173.9 (6)
B(23)-Sn(2)-N(2)-C(211)	57.1 (6)	B(24)-Sn(2)-N(2)-C(29)	-32.7 (8)
B(24)-Sn(2)-N(2)-C(210)	-151.7 (6)	B(24)-Sn(2)-N(2)-C(211)	91.5 (7)
B(25)-Sn(2)-N(2)-C(29)	2.9 (8)	B(25)-Sn(2)-N(2)-C(210)	-116.1 (6)
B(25)-Sn(2)-N(2)-C(211)	127.1 (7)	N(2)-Sn(2)-C(21)-Si(3)	118.8 (6)
N(2)-Sn(2)-C(21)-C(22)	-119.2 (6)	N(2)-Sn(2)-C(21)-B(25)	4.1 (8)
N(2)-Sn(2)-C(21)-B(26)	-56.9 (6)	N(2)-Sn(2)-C(22)-Si(4)	-115.4 (5)
N(2)-Sn(2)-C(22)-C(21)	114.0 (6)	N(2)-Sn(2)-B(23)-C(22)	174.9 (4)
N(2)-Sn(2)-B(23)-B(24)	62.0 (6)	N(2)-Sn(2)-B(23)-B(26)	116.2 (6)
N(2)-Sn(2)-B(24)-B(23)	-124.7 (6)	N(2)-Sn(2)-B(24)-B(25)	121.8 (4)
N(2)-Sn(2)-B(24)-B(26)	178.7 (5)	N(2)-Sn(2)-B(25)-C(21)	177.6 (4)
N(2)-Sn(2)-B(25)-B(24)	-64.6 (4)	N(2)-Sn(2)-B(25)-B(26)	-118.4 (5)
Sn(2)-N(2)-C(211)-C(212)	46.9 (8)	C(29)-N(2)-C(211)-C(212)	163.7 (7)
C(210)-N(2)-C(211)-C(212)	-75.3 (8)	N(2)-C(211)-C(212)-Fe(2)	171.3 (6)
N(2)-C(211)-C(212)-C(213)	-98 (1)	N(2)-C(211)-C(212)-C(216)	79 (1)

Bond Lengths for VII

Sn-C(1)	2.640 (7)	Sn-C(2)	2.653 (7)	B(3)-B(4)	1.684 (12)	B(3)-B(6)	1.803 (12)
Sn-B(3)	2.436 (9)	Sn-B(4)	2.380 (8)	B(4)-B(5)	1.690 (11)	B(4)-B(6)	1.742 (11)
Sn-B(5)	2.468 (8)	Sn-N(1)	2.638 (6)	B(5)-B(6)	1.788 (11)	C(9)-N(1)	1.333 (9)
Sn-N(2a)	2.589 (6)	C(1)-C(2)	1.484 (10)	C(9)-N(2)	1.310 (9)	N(1)-C(10)	1.335 (10)
C(1)-B(5)	1.580 (10)	C(1)-B(6)	1.733 (10)	C(10)-C(11)	1.378 (12)	C(11)-C(12)	1.369 (12)
C(1)-Si(1)	1.869 (7)	C(2)-B(3)	1.600 (11)	C(12)-N(2)	1.343 (10)		
C(2)-B(6)	1.732 (11)	C(2)-Si(2)	1.854 (9)				

Bond Angles for VII

C(1)-Sn-B(3)	60.1 (2)	C(1)-Sn-B(4)	62.1 (2)	Sn-B(4)-C(2)	64.1 (3)	Sn-B(4)-B(3)	71.3 (4)
C(1)-Sn-B(5)	35.8 (2)	C(1)-Sn-N(1)	147.9 (2)	Sn-B(4)-B(5)	72.5 (4)	Sn-B(4)-B(6)	101.2 (4)
B(3)-Sn-B(4)	40.9 (3)	B(3)-Sn-B(5)	66.2 (3)	B(3)-B(4)-B(5)	105.1 (6)	B(3)-B(4)-B(6)	63.5 (5)
B(3)-Sn-N(1)	88.3 (2)	B(4)-Sn-B(5)	40.7 (3)	B(5)-B(4)-B(6)	62.8 (5)	Sn-B(5)-C(1)	78.0 (4)
B(4)-Sn-N(1)	91.2 (2)	B(5)-Sn-N(1)	129.2 (2)	Sn-B(5)-C(2)	63.8 (3)	Sn-B(5)-B(4)	66.8 (4)
Sn-C(1)-C(2)	74.2 (4)	Sn-C(1)-B(3)	56.0 (2)	Sn-B(5)-B(6)	96.6 (4)	C(1)-B(5)-B(4)	105.1 (6)
Sn-C(1)-B(4)	54.0 (2)	Sn-C(1)-B(5)	66.2 (4)	C(1)-B(5)-B(6)	61.6 (5)	B(4)-B(5)-B(6)	60.1 (5)
Sn-C(1)-B(6)	92.1 (4)	Sn-C(1)-Si(1)	127.6 (3)	C(1)-B(6)-C(2)	50.7 (4)	C(1)-B(6)-B(3)	92.2 (5)
C(2)-C(1)-B(5)	112.8 (6)	C(2)-C(1)-B(6)	64.6 (5)	C(1)-B(6)-B(4)	96.7 (5)	C(1)-B(6)-B(5)	53.3 (4)
C(2)-C(1)-Si(1)	129.3 (5)	B(5)-C(1)-B(6)	65.1 (5)	C(2)-B(6)-B(3)	53.8 (4)	C(2)-B(6)-B(4)	97.4 (5)
B(5)-C(1)-Si(1)	117.9 (5)	B(6)-C(1)-Si(1)	139.1 (5)	C(2)-B(6)-B(5)	92.9 (5)	B(3)-B(6)-B(4)	56.7 (5)
C(1)-C(2)-B(3)	111.4 (6)	C(1)-C(2)-B(6)	64.7 (5)	B(4)-B(6)-B(5)	96.5 (5)	B(4)-B(6)-B(5)	57.2 (4)
C(1)-C(2)-Si(2)	132.1 (6)	B(3)-C(2)-B(6)	65.4 (5)	N(1)-C(9)-N(2)	127.8 (6)	Sn-N(1)-C(9)	119.7 (4)
B(3)-C(2)-Si(2)	116.1 (5)	B(6)-C(2)-Si(2)	131.9 (5)	Sn-N(1)-C(10)	122.5 (5)	Sn-N(1)-C(11)	150.0 (3)
Sn-B(3)-C(1)	63.9 (3)	Sn-B(3)-C(2)	79.2 (4)	Sn-N(1)-N(2)	143.7 (3)	C(9)-N(1)-C(10)	115.6 (6)
Sn-B(3)-B(4)	67.7 (4)	Sn-B(3)-B(6)	97.3 (4)	N(1)-C(5)-C(11)	121.3 (7)	C(10)-C(6)-C(12)	118.2 (8)
C(2)-B(3)-B(4)	105.2 (6)	C(2)-B(3)-B(6)	60.9 (5)	C(11)-C(12)-N(2)	121.2 (7)	C(9)-N(2)-C(12)	115.9 (6)
B(5)-B(3)-B(6)	59.8 (5)	Sn-B(4)-C(1)	63.9 (2)				

Torsion Angles for VII

N(1)-Sn-B(4)-B(5)	160.7 (4)	N(2a)-Sn-B(4)-B(5)	98.7 (4)
N(1)-Sn-B(4)-B(3)	-86.0 (4)	N(2a)-Sn-B(4)-B(3)	-148.0 (4)
B(4)-Sn-N(1)-C(9)	-105.4 (5)	B(4)-Sn-N(2a)-C(9a)	-87.3 (5)
C(9)-C(9a)-N(1a)-C(10a)	179.7 (6)	C(9)-C(9a)-N(2a)-C(12a)	179.2 (6)
C(9)-N(1)-C(10)-C(11)	-1 (1)	C(9)-N(2)-C(12)-C(11)	-2 (1)
N(1)-C(9)-C(9a)-N(1a)	+180.0 (6)	N(1)-C(9)-C(9a)-N(2a)	0.9 (9)
N(1)-C(9)-N(2)-C(12)	-0 (1)	N(1)-C(10)-C(11)-C(12)	-1 (1)
N(2)-C(9)-N(1)-C(10)	1 (1)	N(2)-C(12)-C(11)-C(10)	2 (1)

Table IV. Selected Structural Parameters of the Crystallographic Forms of Molecule IV[a]

parameter	molecule 1	molecule 2
N-Sn-B(4)-B(6)[b]	168.1	178.7
N-Sn-B(4)[c]	87.5	89.9
Δ[d]	0.26	0.20
Sn-N[e]	2.557	2.613
Sn-C(12)[e]	3.468	3.286
Sn-C(13)[e]	3.492	3.387

[a] Abstracted from Table III and supplementary material (see Figure 1 for numbering scheme). [b] Torsion angle in deg. [c] Bond angle in deg. [d] Δ = (Sn-C(cage)) - (Sn-B(4)) bond distances in Å. [e] Bond distances in Å.

but similar to that found for 1-Sn(THF)-2,3-$(Me)_2$-2,3-$C_2B_9H_9$ (0.30 Å).[10] Since the Sn-N bond distances in IV are slightly longer than those found in the stannacarborane-2,2′-bipyridine complexes, indicating a weaker interaction, and only one Sn-N bond is formed, the smaller slip distortions in IV are not surprising.[22,23] It is of interest to note that the ferrocenyl group is not in a position of minimum steric interaction with the stannacarborane but is rotated in such a way that the lower half of the cyclopentadienyl ring is fairly close to the cage tin (see Figure 2).[21] Indeed, the tin-cyclopentadienyl rings are within the van der Waals distances in both molecules 1 and 2 (see Table VI). In fact, in molecule 2, which has the longer Sn-N bond, the cyclopentadienyl ring is closer to the tin than in molecule 1. At this point it is not known what, if any, relationship exists between the ferrocenylalkylamine base orientation and the different structural features found in molecules 1 and 2. These are currently under investigation.[21]

The structure of VII is shown in Figure 3. The coordination geometry of each tin is quite similar to that found in the corresponding 2,2′-bipyridine complex.[7] The tin

(23) Barreto, R. D.; Fehlner, T. P.; Hosmane, N. S. *Inorg. Chem.* **1988**, *27*, 453.

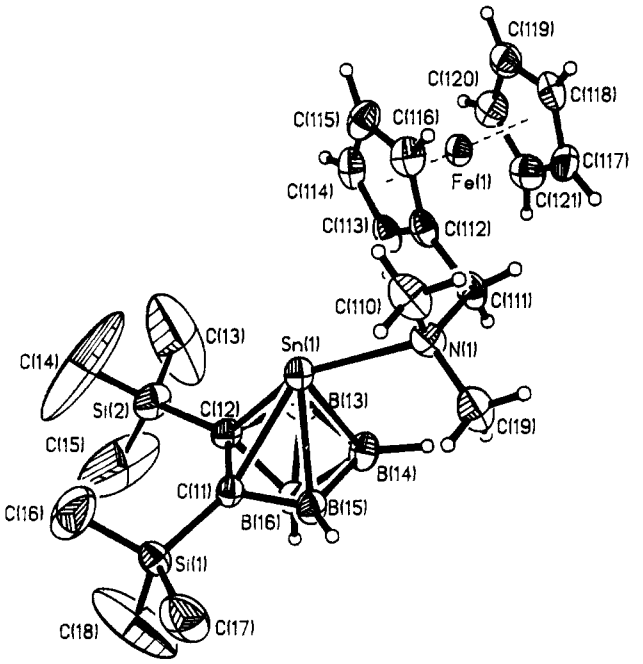

Figure 1. A perspective view of molecule 1 of *closo*-1-Sn[(η^5-C_5H_5)Fe(η^5-$C_5H_4CH_2(Me)_2N$)]-2,3-$(SiMe_3)_2$-2,3-$C_2B_4H_4$ (IV), with thermal ellipsoids drawn at 30% probability level and showing the atom numbering scheme.

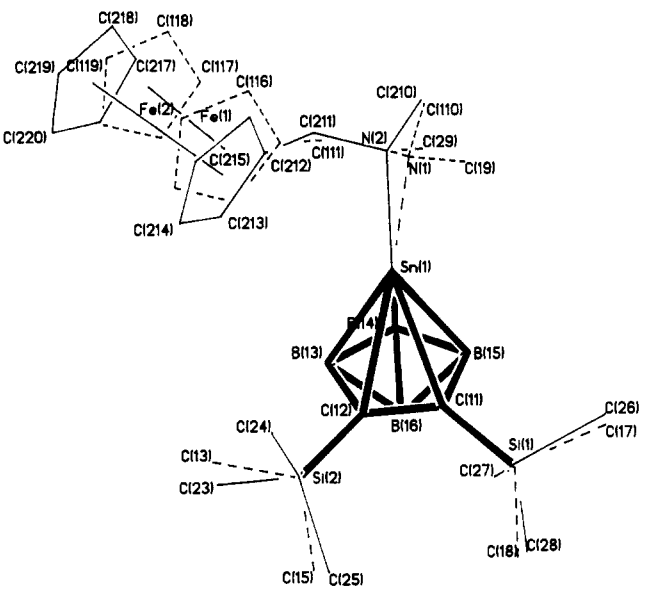

Figure 2. Superimposed line drawings of the two crystallographically independent molecules of IV. Thick darkened lines represent almost identical geometries of the carborane cages, while broken and unbroken thinner line drawings represent nonsuperimposed Lewis bases in molecules 1 and 2, respectively.

atoms are slipped toward the unique boron in the C_2B_3 face of the carborane with the resulting Sn–C(cage) distance [2.646 (7) Å] being 0.266 Å longer than the Sn–B(unique) distances [2.380 (8) Å]. The bipyrimidine base in VII is directly opposite the cage carbons, and the bipyrimidine rings are at a dihedral angle of 44.21 (3)° with the C_2B_3 faces of the carboranes. In the $(C_{10}H_8N_2)Sn(SiMe_3)_2C_2B_4H_4$ difference between the Sn–C(cage) and Sn–B(unique) bond distances is 0.38 Å and the dihedral angle between the bipyridine rings and the C_2B_3 face is 26.8 (5)°.[7] Recent MNDO–SCF calculations[22] on the model compound $(C_{10}H_8N_2)SnC_2B_4H_6$ showed that the Sn bonds to the carboranes primarily through the Sn(4p) orbitals, one directed radially toward the carborane and the other

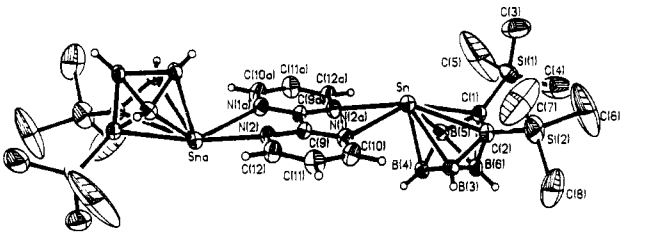

Figure 3. Structure of 1,1′-(2,2′-$C_8H_6N_4$)-[*closo*-1-Sn-2,3-$(SiMe_3)_2$-2,3-$C_2B_4H_4]_2$ (VII) showing the trans configuration of the stannacarboranes with the atom numbering scheme and thermal ellipsoids at the 30% probability level. The midway between C(9)–C(9a) bond lies at a center of symmetry.

Table V. MNDO–SCF Results for *cis*- and *trans*-1,1′-(2,2′-$C_8H_6N_4$)-[*closo*-1-Sn-2,3-$C_2B_4H_6]_2$

property	trans	cis
symmetry	C_{2h}	C_{2v}
$\Delta H_f°$, kcal/mol	148.413	150.124
ionization potential, eV	9.601	9.530
dipole moment, D	1.140	16.128
Sn–C(cage), Å	2.513	2.521
Sn–B(4), Å	2.273	2.269
Sn–N, Å	2.478	2.491
B(4)–B(4)′, Å	8.133	6.497
B(3/5)–B(3/5)′, Å	9.084	8.269
Sn–Sn′, Å	6.509	6.537
dihedral angle,[a] deg	20	22

[a] Dihedral angle between the bipyrimidine rings and the C_2B_3 carborane face.

two directed tangentially parallel to the carborane face. The two tangentially directed orbitals are also those mainly involved in tin–bipyridine bonding. The most efficient bonding between the tin and the Lewis bases would be expected when the bipyridine rings and the C_2B_3 face were parallel (a dihedral angle of zero). However, repulsion between the two ligands prevents this orientation. The increased slippage of the apical tin in stannacarborane on complexation with the Lewis base was shown to be the result of a decrease in Sn–C(cage) bonding and relief of ligand–ligand repulsion, thereby allowing a more parallel orientation of the bipyridine rings and the carborane face. On the basis of such an analysis one would expect that for Lewis bases of similar structure, a stronger base–tin interaction would result in an increased slippage of the tin and smaller base–carborane dihedral angles. This is precisely what is found in VII. The weaker bipyrimidine base (especially when coordinated to another tin) produces a complex with less slippage and an increased dihedral angle. MNDO–SCF calculations were carried out on the model compound *trans*-1,1′-(2,2′-$C_8H_6N_4$)-[*closo*-1-Sn-2,3-$C_2B_4H_6]_2$. Table V summarizes some calculated parameters and pertinent bond distances. The calculations show that tin–carborane and tin–base interactions are essentially the same as found in the 2,2′-bipyridine system and need not be repeated here. However, two aspects of the bipyrimidine system (compounds VII, VIII, and IX) are worth commenting on. The first is the essentially exclusive formation of the bimetallic complexes even in the presence of excess bipyrimidine, and the second is trans orientation of the stannacarboranes about the bipyrimidine ring.

MNDO–SCF calculations show that reaction 1 would have a $\Delta H° = 20.5$ kcal/mol. This value was obtained

$$2(C_8H_6N_4)SnC_2B_4H_6 \rightarrow (C_8H_6N_4)(SnC_2B_4H_6)_2 + C_8H_6N_4 \quad (1)$$

from the calculated values of $\Delta H_f°$ for the relevant compounds in the reaction. Even though this is a calculated value for the gas phase reaction, it does indicate that there

is no inherent gain in stability, at least as measured by ΔH, on forming the bimetallic complex. The absence of any monostannacarborane–bipyrimidine is most likely due to the preparative procedure. The complexes were purified by sublimation, and it is likely that any monostannacarborane product formed would decompose during sublimation to give the less volatile bimetallic compound. It should be noted that the NMR spectral or spectroscopic data reported in the Experimental Section were obtained on solutions of the purified bimetallic complex dissolved in C_6D_6.

The trans orientation of the stannacarboranes in VII seems to be dictated on steric grounds. Table V lists some calculated optimized parameters for the cis isomer of the model compound. Calculations show that there is very little energy difference between the two isomers (≈2 kcal/mol). The cis isomer has slightly longer Sn–N bonds, an increased slippage of the Sn, and a larger dihedral angle than the trans isomer. Although the differences are small, they are consistent with a higher repulsion between the stannacarborane units in the cis isomer. The individual atomic interactions can be analyzed by partitioning the total energy of the molecules into a series of one- and two-center energy terms.[24,25] Such a partitioning was found to be useful in explaining the geometry of the $(C_{10}H_8N_2)SnC_2B_4H_6$ complex.[22] A comparison of the two center terms in the cis and trans complexes shows that an increase in repulsion between the unique borons of the carboranes is found in going from the trans to the cis isomer (see Table V for interatomic distances). The small energy difference between the two isomers indicates that there should be an easy conversion between the two forms. Indeed, the solution spectral data presented (see Experimental Section) for compounds VII, VIII, and IX could be that of a mixture of the two isomers. From the differences in dipole moments shown in Table V, it may be possible to isolate the cis complex by recrystallization from a polar solvent.

Acknowledgment. This work was supported by grants from the National Science Foundation (CHE-8800328), the Robert A. Welch Foundation (N-1016), and the donors of the Petroleum Research Fund, administered by the American Chemical Society. We thank Dr. Charles Campana (Nicolet Instruments Corp.) and Professor Larry Dahl (University of Wisconsin at Madison) for their help in obtaining the crystal structure of VII.

Registry No. I, 90388-43-5; II, 91670-63-2; III, 91686-40-7; IV, 120829-86-9; V, 120829-83-6; VI, 120829-84-7; VII, 110374-95-3; VIII, 120853-36-3; IX, 120829-85-8.

Supplementary Material Available: Listings of mass spectrometric data (Table S-I) and IR absorptions (Table S-II) of IV, V, VI, VII, VIII, and IX, tables of anisotropic displacement coefficients of IV (Table S-III) and VII (Table S-VII), additional tables of bond lengths, bond angles, and torsion angles for IV (Table S-IV) and VII (Table S-VIII), tables of H-atom coordinates and isotropic displacement coefficients for IV (Table S-V) and VII (Table S-X), and a table of deviations of the atoms from the plane formed by C_2B_3 and bipyrimidine ring (Table S-IX) for VII (24 pages); listings of structure factors of IV (Table S-VI) and VII (Table S-IX) (40 pages). Ordering information is given on any current masthead page.

(24) Dewar, M. J. S.; Lo, D. H. J. Am. Chem. Soc. **1971**, *93*, 7201.
(25) Olivella, S.; Vilarrusa, J. *J. Heterocycl. Chem.* **1981**, *18*, 1189.

UV Photoelectron Spectra and Electronic Structure of 1,2-Diosmacyclopropane and 1,2-Diosmacyclobutane Complexes

Bruce R. Bender,[1a] Renzo Bertoncello,[1b] Michael R. Burke,[1d] Maurizio Casarin,[1c] Gaetano Granozzi,*[1b] Jack R. Norton,*[1a] and Josef Takats*[1d]

Department of Chemistry, Colorado State University, Fort Collins, Colorado 80523, Dipartimento di Chimica Inorganica, Metallorganica ed Analitica, Università di Padova, via Loredan 4, 35131 Padova, Italy, Istituto di Chimica e Tecnologia dei Radioelementi del CNR, Padova, Italy, and Department of Chemistry, University of Alberta, Edmonton, Alberta, Canada, T6G 2G2

Received February 22, 1989

The electronic structures of two isolobal analogues of cyclopropane and cyclobutane, $Os_2(CO)_8(\mu\text{-}CH_2)$ and $Os_2(CO)_8(\mu\text{-}C_2H_4)$, have been investigated by means of gas-phase UV photoelectron (PE) spectroscopy and DV–Xα MO calculations. A comparison between the bonding schemes of the organic and organometallic partners reveals that the qualitative features of the bonding in these molecules are in accord with the concept of the isolobal analogy. However, differences are found when a quantitative description of the bonding is attempted since the metal complexes contain an additional framework MO with significant Os–C antibonding character. This feature is due to the involvement of the t_{2g}-like MOs of the metallic fragments with the interactions within the dimetallacycle. The UV–PE data lend support to the picture arising from the theoretical calculations.

Introduction

In recent years Hoffmann[2] has elegantly and exhaustively demonstrated the value of comparing the frontier orbitals of various metal–ligand combinations with those of hydrocarbon fragments (CH_3, CH_2, and CH). Stone[3] has also very successfully used this "isolobal connection" to guide the preparative work on, and to rationalize the structures of, complexes containing metal–metal bonds. The triangulo $M_3(CO)_{12}$ clusters (M = Ru, Os) can be

(1) (a) Colorado State University. (b) University of Padova. (c) CNR of Padova. (d) University of Alberta.
(2) Hoffmann, R. *Angew. Chem., Int. Ed. Engl.* **1982**, *21*, 711.
(3) Stone, F. G. A. *Angew. Chem., Int. Ed. Engl.* **1984**, *23*, 89.

0276-7333/89/2308-1777$01.50/0